

Characterising the wake of horizontal axis marine current turbines

A.S.Bahaj¹, L.E.Myers¹, M.D. Thomson² & N. Jorge³

¹Sustainable Energy Research Group, School of Civil Engineering and the Environment,
University of Southampton, Southampton SO17 1BJ, UK.
E-mail: serg@soton.ac.uk

²Garrad Hassan and Partners Limited, St. Vincent's Works,
Silverthorne Lane, Bristol, BS2 0QD, UK
E-mail: mat.thomson@garradhassan.com

³Garrad Hassan, Portugal
E-mail: nuno.jorge@garradhassan.com

Abstract

This paper presents a discussion on the characterisation of the wake of horizontal axis marine current turbines. Understanding the effect devices have on the flow is critical in determining how one device may modify both the performance of and loading experienced by another device in a farm or array. It is the aim of this work to identify and investigate the parameters which govern the wake structure and its recovery to the free-stream velocity profile. An experimental and theoretical investigation of the flow field around small-scale mesh disc rotor simulators is presented. Wake characteristics of the rotor simulators have been measured in the 21m tilting flume at the Chilworth hydraulics laboratory, University of Southampton. The experimental results are at present being used to develop a numerical wake model for Marine Current Energy Converter (MCEC) devices. Based on an industry standard wind turbine wake model, developed by Garrad Hassan over the last 15 years, an eddy-viscosity model is presently being developed to model device wakes.

This work has been conducted as part of a DTI-funded project to develop a tool which will assist in the layout design of arrays, ensuring they are optimally spaced and arranged to achieve the maximum possible energy yield at a given tidal energy site.

Keywords: eddy-viscosity, modelling, turbine, wake

Nomenclature

a = axial induction factor
 A = area
 C_t = rotor thrust coefficient
 d = depth
 D = diameter (of rotor disk)
 E = eddy-viscosity

Fr = Froude number
 g = gravitational constant
 h = rotor hub height
 I = turbulence intensity (in the x-direction)
 m = meters
 L = Length
 Re = Reynolds number
 u = axial component of velocity
 U = stream wise velocity (x-direction)
 v = radial component of velocity
 uv = Reynolds stress
 X = scale factor
 ν = kinematic viscosity
 ρ = fluid density

Subscripts

0 = free stream at hub height
amb = ambient condition
m = model
p = prototype
r = radial direction
w = wake
x = axial direction
y = lateral direction
z = vertical direction

Superscripts

– = mean value

1 Introduction

Marine current energy conversion technology is presently at the prototype stage where single devices are deployed, or planned for installation, at isolated testing sites. The large marine current energy resource around the world tends to be concentrated at relatively compact sites where tidal flows are spatially constrained such as between islands, around headlands or estuarine-type inlets [1]. If MCECs are to achieve viable costs of electricity generation devices will have to be installed in arrays at such sites. Understanding the effect devices have on the flow is critical in determining how one device may modify both the performance of, and loading experienced by, another device in the array. Hence, investigations characterising the wake of an MCEC device are required. It is the aim of this work to identify and investigate the parameters which govern the wake structure and its recovery to the free-stream velocity profile.

Although MCECs may appear similar to modern wind turbines, the design of an MCEC array may be appreciably different, predominantly due to:

- Decreased lateral spacing (perpendicular to flow). Many sites with strong tidal flows have bi-directional flow characteristics, thus the lateral spacing of devices could be reduced. However, there will be a limit to this spacing to prevent detrimental downstream wake interactions; and
- Staggered or increased row spacing. Devices will need to be located far enough downstream to ensure that both the free-stream flow velocity is recovered and that turbulence levels are not excessive.
- Proximity to flow boundaries. Rotors are expected to sweep close to the sea bed and water surface (compared to wind turbine operation) in a fluid that typically may only be twice the rotor diameter in height.

Understanding the development of the wake and its dissipation downstream is critical in optimising array layout. The wake structure downstream of a horizontal axis wind turbine is well understood and has been investigated using both small-scale actuator disc experiments, larger models and full-scale turbines. However, underwater conditions are sufficiently different and will require additional investigations, specifically to account for the change in fluid and the presence of a bounding free surface.

This paper reports on the initial finding of experiments used to investigate and characterise the far wake region of MCEC devices. The results of these experiments will be used to develop a numerical model that can predict the structure and recovery of the wake.

2 Characterisation of the wake

Any device that extracts energy from a flow causes a reduction in the momentum of the downstream flow. The flow affected by the device is defined as the wake. The specific form of a wake is likely to be complicated and device specific. However, the fundamental physics

governing the wake structure and its dissipation can be simplified by considering the wake as two distinct regions:

Near wake

Extracting momentum from the flow, whilst conserving mass, drives a wake expansion. This usually occurs within 0-1 diameters (D) downstream. In addition is likely that the MCEC will convert the extracted energy into some form of mechanical motion. This may take the form of vortices shed from the blade tips and from the device support structure and will bound the slower moving flow from the free-stream flow. These vortices create a discontinuity in the stream velocity profile. Typically the near wake exists from 0-3/4 D , in which time the ambient turbulence of the free-stream flow breaks down the bounding vortices.

Far wake

Once the initial conditions for the far wake are established by the near wake region there are two main mechanisms that drive the wake structure. These are convection and turbulent mixing. If the fluid were completely inviscid then a volume of slower moving flow would just convect downstream at a slower rate than the free-stream flow. However, turbulent mixing is present and acts to re-energise the wake, breaking it up and increasing the velocity until, at a point far downstream the velocity profile approaches that which existed upstream of the rotor.

3 Features affecting the wake

There are many factors that can affect the wake region. Some of these are shown in figure 1. The principle features are discussed below:

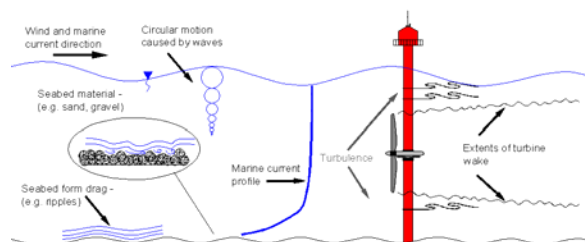


Figure 1: Some variables that will affect device performance and wake structure.

Device performance

The extraction of energy from the flow will cause a change in momentum across the rotor disk. The magnitude of this change in momentum will affect the initial velocity deficit within the wake. A common non-dimensional value used to quantify the change in momentum caused by a device is the thrust force coefficient (C_t). Some early literature regarding the momentum change across wind turbines [2] assumed a constant value of C_t , but later work attempting to characterise the centreline downstream velocity of a 1/30th scale MCEC [3] highlighted the

significance of accounting for device thrust. The initial wake velocity behind a horizontal axis rotor can be directly related to C_t by using actuator disc theory

$$C_t = \frac{\text{thrust}}{0.5\rho U_0^2 A} = 4a(1-a) = 1 - \left(\frac{U_w}{U_0}\right)^2 \quad (3.1)$$

Ambient and device generated turbulence

Marine turbulence can be generated from a variety of different sources yielding turbulent flow structures of varying length scales. Sea bed material, ripples, bed forms and changes in bathymetry are the principle drivers at lower depths. Waves and swell will cause turbulence towards the surface with length scales that decrease in a logarithmic manner with increasing depth. Turbulence generated by the ambient environment will promote wake mixing far downstream of the turbine. Additional turbulence will be generated from the MCEC device itself such as vortices shed from the blades and support structure. This will dissipate in the near-wake region.

Bounding surfaces

Early MCEC devices are likely to be situated in relatively shallow water depths of 30m or less. A typical 1MW device located mid-depth is likely to create a wake that will be affected by the proximity of the both the sea bed and the free surface. The presence of two bounding surfaces acts to restrict the flow vertically forcing greater lateral motion (known as blockage). This results in the loss of three-dimensional symmetry.

Free surface

The presence of a free surface allows the depth to vary and requires the consideration of gravity or Froude (Fr) effects:

$$Fr = \frac{U}{\sqrt{g d}} \quad (3.2)$$

There are two possible effects on the wake: a) local fluctuation can generate near surface ambient turbulence (see above); b) the extraction of energy from a flow must result in a channel head drop. For a single device in a large channel this drop is very small. However, such effects may be exacerbated in arrays, which could lead to significant changes in depth downstream of a row of MCECs. A drop in depth has two effects a) an increase in flow speed (see note on flow speed below) and b) an increase in flow blockage. There is some evidence that small clearance between the rotor and the water surface may affect device performance [4] in terms of decreasing power production whilst rotor thrust remains unchanged. Such effects require investigation if operation close to flow boundaries are realised at full-scale.

Sea bed boundary layer

Due to the likely proximity of an MCEC to the sea bed it is expected that the wake will be affected by the sea bed boundary layer. There are a number of different equations used to model the velocity profile due to the presence of a

boundary layer. Some utilize a simple power law [5] that may extend either from sea bed to surface or from bed to half depth, with the upper portion of the water column assigned a constant velocity [6]. Other methods incorporate the sea bed roughness [7] as a variable to more accurately define the velocity in the lower part of the water column. There are also field measurements of vertical velocity profiles [8] which show a close correlation to the above expressions. The shear characteristics of the velocity profile may affect the wake formation as disproportionate amounts of flow pass above and beneath the rotor disc. The velocity gradient may also affect wake mixing rates downstream of the rotor.

Free-stream flow speed.

The faster the free stream moves the greater the convection of the wake (i.e. the further downstream the wake is carried in the same time period). The free stream speed is therefore a key parameter in evaluating the wake velocity.

The general expression below can be used to describe the parameters that are likely to impact on the wake velocity:

$$U_w = f(U_0, C_t, I_{\text{amb}}, d, h, x) \quad (3.3)$$

4 Experimental scaling

Modelling horizontal axis rotors becomes impractical at very small scale. Accurately scaling the channel flow properties whilst maintaining rotor thrust, power and tip speed is not possible without changing aspects of the downstream flow field. For instance, accurate tip speed scaling would require a 100mm diameter model rotor to have a rotational rate in excess of 1500RPM. This is clearly unachievable from a design point of view and would add a great deal of swirl and induce large pressure gradients to the wake. Since swirl and similar effects generally dissipate a short distance downstream of the rotor it is thought that the accurate reproduction of the thrust exerted on the rotor is of principle importance. This thrust can be provided by static mesh disc rotor simulators that have the correct size for appropriate hydraulic scaling of the flow properties and have varying thrust coefficients through the level of porosity. Far wake characteristics are assumed to be similar to that of full-scale rotors due to parity between accurately scaled rotor thrust and channel flow properties. There is also evidence of previous investigations [9, 10] concerning the study of flow fields around horizontal axis rotors using mesh disc simulators.

This work can be conducted quickly, covering a wide range of variables and performed without the time constraints encountered at expensive larger scale facilities. Model simulator work will also identify the variables that have the most important effects upon the flow profile in a channel helping to structure subsequent rotor testing.

The use of mesh disc simulators will not have the same influence upon the flow as a standard rotor. The principle differences are:

- i. The energy extracted from the flow is converted to small-scale turbulence downstream of the disc as opposed to being extracted as mechanical motion.
- ii. Vortices shed from the edges of the disc will differ from those of a rotating blade.
- iii. The swirl angle of the flow from the mesh disc will be zero.

All these effects are expected to be exclusive to the near-wake region less than 4 diameters downstream of the rotor disc [11, 12]. This has been confirmed for this work during flow visualisation work conducted prior to testing.

Testing was conducted in the University of Southampton 21m tilting flume at the Chilworth research laboratory. The flume is 1.37m wide, 21m in length, maximum depth of 0.5m and peak flow rate of 2.3 m³/s. Mesh discs were constructed at 100mm diameter and a range of porosities (ratio of open to closed area). At a typical flow depth of 300mm this gave a blockage ratio (occupied/flow area) of around 2%.

Scaling properties of an open channel can present problems. Froude (Fr) and Reynolds (Re) numbers cannot be linearly scaled together when the model/prototype ratio becomes too small. The Froude number must be kept constant between model and prototype such that:

$$Fr_r = \frac{U_r}{\sqrt{g_r L_r}} = 1 \quad (4.1)$$

So for a 1/Xth scale model:

$$\frac{L_m}{L_p} = \frac{1}{X} \quad \text{and} \quad \frac{U_m}{U_p} = \frac{1}{X^{1/2}} \quad (4.2)$$

Figure 2 shows the range of Froude numbers used during the testing period alongside a typical range expected for 30m deep tidal channel. It can be seen that for the shallow depths usually encountered in flumes Froude numbers become too great if flow speeds are to be achieved that can provide suitable velocities to turn a horizontal axis rotor. Drop lines on the graph illustrate the typical model scale Froude numbers used during this work and the full-scale flow speeds that they represent. All are close to the expected rated flow speeds of prototype and mature technology full-scale devices.

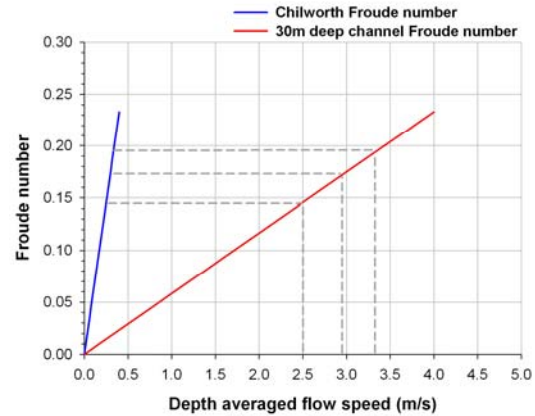


Figure 2: Froude number scaling relationship between Chilworth flume testing and typical full-scale site.

Reynolds number scaling cannot be achieved in normal practice if the same fluid is used in model and prototype. For the channel the Reynolds number is defined as

$$Re = \frac{UL}{\nu} \quad (4.3)$$

Where L is characteristic length here expressed as the hydraulic mean depth of the flow. In a channel of uniform section this is equal to the depth. Discrepancy in Reynolds numbers between model and prototype is usually tolerated for the scaling of hydraulic channels if:

- a) Froude similarity is maintained
- b) Both full-scale and model Reynolds numbers lie within the same turbulent classification

As one might expect, full-scale Reynolds numbers for a tidal channel are high, in the order of 10⁷ and therefore fully turbulent. The transition to turbulent flow occurs at Reynolds numbers of approximately 2×10³ and thus experimental conditions in the Chilworth flume are well within the turbulent region.

5 Experimental Methodology

Mesh disc rotor simulators were suspended from a load cell rig via a stainless steel support arm (Figure 3).

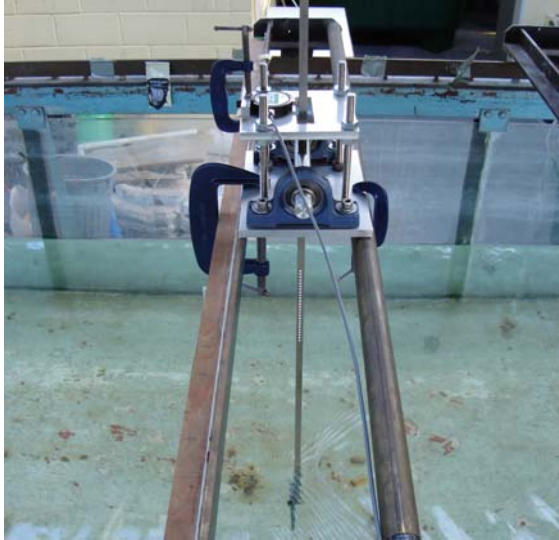


Figure 3: Mesh disc support rig. Button load cell can be seen at top, submerged mesh disc visible at base of image.

A 10N load cell was used to measure the thrust exerted by the mesh disc upon the flow and thus calculate the disc thrust coefficient. A pivot arrangement was used due to the low disc thrust values anticipated when testing at Froude numbers representative of full-scale conditions. When installed in the Chilworth flume, the mechanical advantage of the pivot arrangement increased the disc thrust by an order of magnitude at the load cell. The load cell was secured to a height-adjustable plate that permitted variation of the disc to pivot / pivot to load cell distance ratio. Load cells were calibrated regularly during testing with zero readings also recorded at regular intervals to allow for changes in temperature. Load cell slope (mV output per unit load) remained perfectly linear and constant throughout the testing period.

Mesh discs were constructed from thin sheet PVC plastic with a number of drilled holes. Porosity (ratio of open to closed area) ranged from 0.48 to 0.35. Higher porosities were achieved by using wire mesh discs. The stainless steel stem used to mount the discs measured 4mm in width, 10mm depth. Material selection was based upon the need to have a narrow profile presented to the incoming flow whilst maximising stiffness.

Flow profiling around the mesh disc rotor simulators was performed using an Acoustic Doppler Velocimeter (ADV). This method of measuring flow properties has increased during the last few years, no doubt due to the ease of use of ADVs, the higher sampling frequencies, reduced sample volumes, device robustness and relatively low cost

compared to laser and hot wire systems. Accuracy of ADV instruments has also been shown to be very good with mean velocity errors less than 1% achievable [13]. The sample period for each measurement point within the disk wake was 60 seconds. At a sampling frequency of 50Hz, this period ensures sufficient data collection is achieved to calculate the representative mean velocities. Figure 4 shows that after 30 seconds the cumulative mean velocity has stabilised. This sample period also ensures that the largest of channel turbulence length scales are sampled.

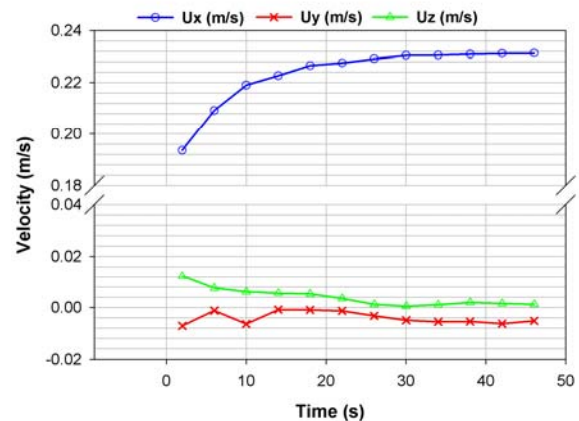


Figure 4: Cumulative mean velocity measurements downstream of a mesh disk simulator.

Turbidity in the flume was high due to a good level of suspended particles and thus the signal to noise ratio (SNR) of the instrument was high throughout the testing period. A value of SNR >15 is generally recommended for good accuracy of instantaneous measurement or high frequency turbulence mapping [14]. SNR values were generally between 18 and 22 for the test results show here. Similarly the device correlation coefficient values (a measure of data quality) was in excess of 90% throughout the testing. The raw data collected was filtered to only include correlation values >95%. The accepted minimum value for filtering is approximately 70%.

In order to provide a detailed view of the flow downstream of the mesh disc a large number of point measurements were taken. The persistence of the wake measurements were taken along the flume centreline from 2.5 to 20 diameters downstream. From 3 to 7 diameters downstream lateral measurements were taken in order to map the expansion of the wake. Finally 8 measurements were taken vertically down through the water column at each location.

Several base flow measurements were also taken in the absence of the disc. A typical measured vertical flow profile is shown in figure 5 alongside other theoretical expressions. It can be seen that the flow profile is well developed and is in agreement with measurements at a full-scale tidal sites [8].

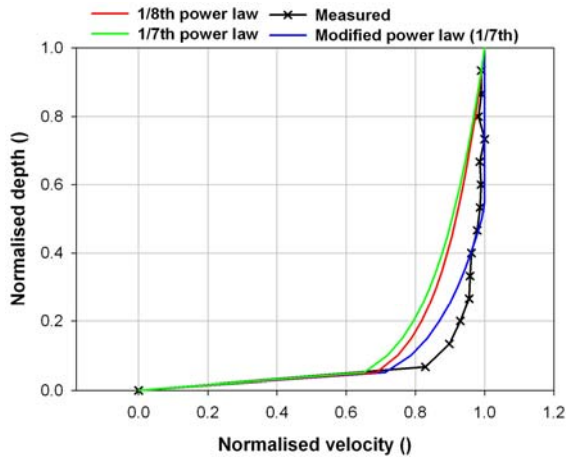


Figure 5: Measured and theoretical vertical velocity profiles for the Chilworth flume.

6 Presentation of results

To gain an understanding of how different factors impact on the far wake flow field, data has been visualised on contour plots. Data points were linearly interpolated to plot a continuous flow. The following figures demonstrate a set of example plots used to compare the velocities and turbulence intensity changes in and around the wake. Channel dimensions are given in terms of disc diameters and blue dots indicate measurement points.

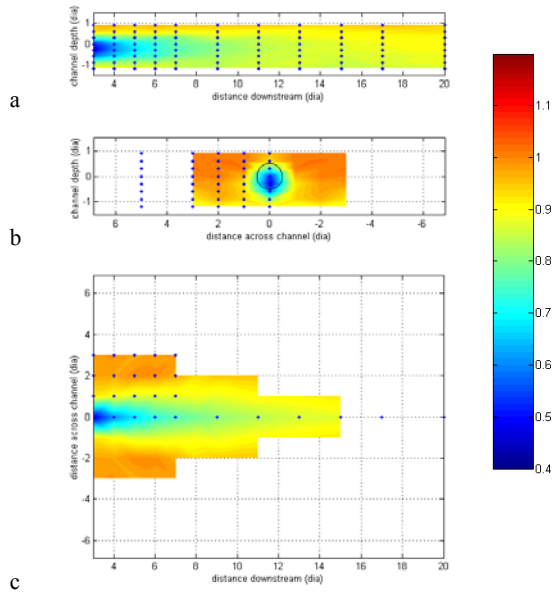


Figure 6: Normalised stream velocity (u/U_0) of the flow downstream of a porous disc of $C_t = 0.95$ in a flow of $U_0=0.333\text{m/s}$ and $Fr. = 0.171$, a) y-slice along the disc centreline b) x-slice at 3D downstream and c) z-slice at $-0.3D$ below the centreline.

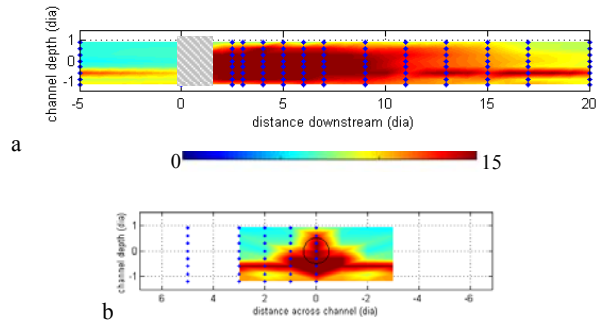


Figure 7: Turbulence intensity % (x-direction) of the flow downstream of a porous disc with $C_t=0.95$ in a flow of $U_0=0.333\text{m/s}$ and $Fr = 0.171$, a) y-slice at centreline and b) x-slice at 3D downstream.

The turbulence intensity (I) is defined as:

$$I \equiv \frac{u'}{U} \quad (6.1)$$

Where u' is the root-mean-square of the turbulent velocity fluctuations and \bar{U} is the mean velocity.

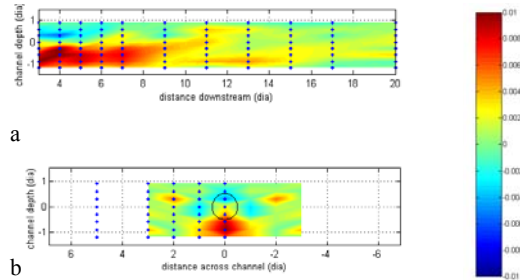


Figure 8: Vertical velocity (w) of the flow downstream of a porous disc with $C_t=0.95$ in a flow with $U_0=0.333\text{m/s}$ and $Fr. = 0.171$, a) y-slice at centreline and b) x-slice at 3D downstream. Scale ± 0.01 m/s

Wake recovery can also be defined in terms of velocity deficit, which is a non-dimensional number relative to the free-stream flow speed at hub height (U_0) and is defined as:

$$U_{\text{deficit}} = 1 - U_w/U_0 \quad (6.2)$$

Figure 9 below demonstrate how the velocity deficit profile varies as the wake recovers. A 100mm diameter disk was positioned at half depth in 300mm deep flow. The depth-averaged flow velocity was 0.331m/s and the disk had a thrust coefficient $C_t=0.95$.

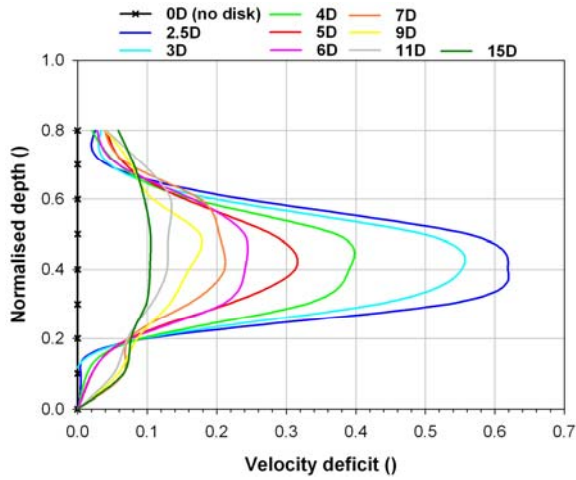


Figure 9: Measured vertical velocity deficit profiles downstream of a porous disc with $C_t = 0.95$, $U_0 = 0.333\text{m/s}$ (depth averaged) $Fr. = 0.171$.

7 Results

General observations from the experiments include:

- Figure 5 shows the stream velocity profile to have a sharp transition boundary layer. This is typical of a turbulent shear layer. Figure 7 confirms the presence of a band of highly turbulent fluid.
- It can be seen in Figure 5a that the bounding free surface restricts the expansion of the wake compared to that of the lateral expansion in Figure 5c. Further tests are required to confirm the continuation of lateral expansion.
- It is apparent in Figures 6, 7 & 8 that the vertical centreline of the wake is not centred on the porous disc. Using the normalised velocity deficit in Figure 9 it appears that the wake centreline is $0.1D$ below the disc centreline. This probably due to a combination of the turbulent shear layer and the bounding free surface forcing a greater proportion of flow over the disc. Further investigations into varying hub height and channel depth are required to characterise this offset.
- The velocity deficit within the wake is clearly demonstrated in Figure 9. The greatest deficit is found just downstream of the disc. With increasing downstream distance the flow profile tends towards the upstream velocity profile. It is interesting to note the persistence of the wake and that even after 20 diameters the flow speed, whilst more uniform, is still only 90% of that upstream of the disc. To remove the effect of the boundary layer the velocity is normalised to the inflow profile. Figure 8a suggests there is a greater up-flow below the wake, which coincides with the turbulent boundary layer and suggests greater mixing.

Specific experiments have investigated the effect of C_t on the wake structure. Figure 10 shows the centreline velocity deficits downstream of various porous discs under constant flow conditions (depth = 300mm, depth-averaged velocity = 0.333m/s , Froude number = 0.171). It is clear that thrust affects the initial conditions of the wake, with an initial deficit similar to that predicted by equation 3.1. The flow conditions are identical for all the tests, suggesting that the near wake region may impart an effect up to 6D downstream. The converging plots demonstrate the general dissipation trend, driven by the ambient turbulence intensity.

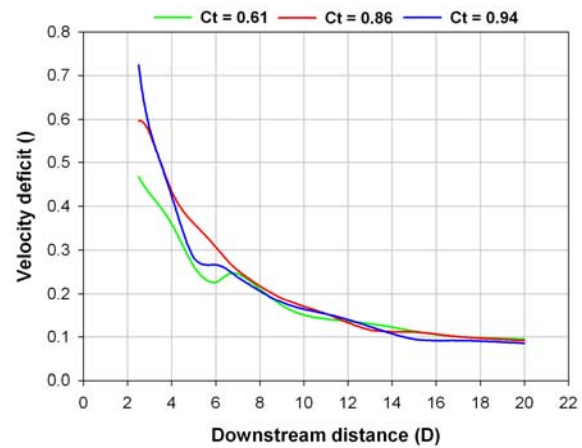


Figure 10: Measured centreline velocity deficit profiles downstream of 3 porous discs under identical flow conditions.

Varying the inflow stream velocity should affect the downstream wake and this is seen clearly in Figure 11, where the wake centreline velocity is dependant on the free-stream flow speed.

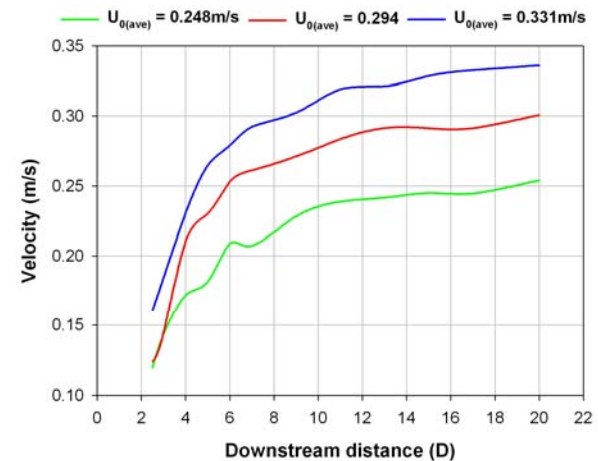


Figure 11: Measured centreline velocity profiles downstream of a porous disc for varying flow speed.

However, the velocity deficit displays (Figure 12) a general recovery trend. This demonstrates that the wake velocity is directly proportional to free stream velocity, yielding the following:

$$U_w = g(C_t, I_{amb}, d, h, x) \cdot U_0$$

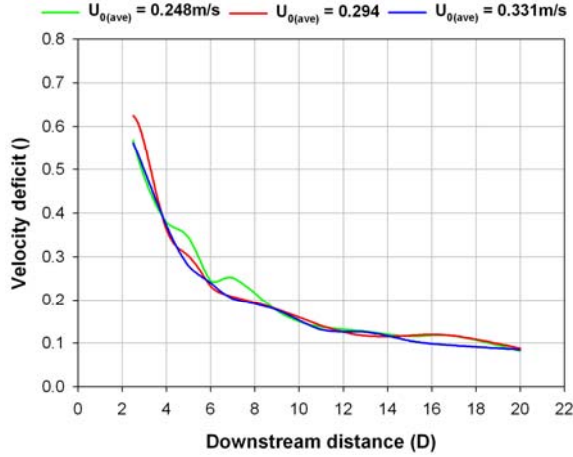


Figure 12: Measured centreline velocity deficit profiles downstream for the same porous disc. Flow conditions vary by flow speed only

8 Eddy-viscosity model

An eddy-viscosity model has been employed to replicate the turbulent mixing process in the wake, whilst observing both the conservation of mass and momentum in the wake. At present this work is ongoing with the initial results expected shortly after the time of writing. The wake velocity deficit field is calculated using a finite-difference solution of the thin shear layer equation of the Navier-Stokes equations in axi-symmetric co-ordinates.

$$u \frac{\partial u}{\partial x} + v \frac{\partial u}{\partial r} = -\frac{1}{r} \frac{\partial(r \overline{uv})}{\partial r} \quad (8.1)$$

An eddy-viscosity, averaged across each downstream wake section, is used to relate the shear stress term in the thin shear equation to gradients of velocity deficit.

$$-\overline{uv} = \varepsilon \frac{\partial u}{\partial r} \quad (8.2)$$

Equation 8.2 permits the shear stress terms in equation 8.1 to be expressed in terms of the eddy viscosity. The governing differential equation to be solved becomes:

$$u \frac{\partial u}{\partial x} + v \frac{\partial u}{\partial r} = \frac{\varepsilon}{r} \frac{\partial(r \partial u / \partial r)}{\partial r} \quad (8.3)$$

The eddy-viscosity value is evaluated using appropriate length-scales in the form:

$$\varepsilon(x) = L_m(x) U_m(x) \quad (8.4)$$

L_m and U_m are suitable length and velocity scales of the turbulence as a function of the downstream distance x but independent of r . A suitable length scale, proportional to the wake width (B_w) is taken. The velocity scale is proportional to the difference $U_0 - U_w$ across the shear layer. Using U_0 as the inflow free-stream velocity profile the sea bed boundary layer is automatically taken into consideration. The presence of ambient turbulence within the flow means that the eddy viscosity in the wake cannot be wholly described by the shear contribution alone but an ambient term is included. Hence the overall eddy viscosity is given by:

$$\varepsilon(x) = F \cdot K \cdot B_w \cdot (U_0 - U_w) + \varepsilon_{amb} \quad (8.5)$$

Where the filter function F is a factor applied for near wake conditions. This filter can be introduced to allow for the build up of turbulence on wake mixing and, as illustrated in Figure 10 is dependant on C_t . The dimensionless constant K is a global field constant to be determined by experiments and ε_{amb} is the ambient eddy viscosity term, also to be determined by experiment.

The presence of the two bounding surfaces breaks the asymmetry of the model. A simple approach to overcome this problem is to decouple the vertical and lateral models. The lateral model yields the unbounded solution, based on the initial conditions of a bounded disc. Where as the vertical model employs the method of images to impose the additional constraints. The method of images repeats the initial velocity deficit profile at position of d above and below the centreline of the porous disc. The Crank Nicholson method is then used to solve a tri-diagonal matrix at the first grid node of the wake, giving the centre line velocity at the next grid point downstream. The calculation propagates downstream evaluating the downstream velocity field.

It is the aim of this initial work to validate two aspects of the eddy-viscosity model: a) the addition of imposed boundary conditions limiting the vertical dissipation; and b) the global field constants for a marine flow.

Initial numerical results so far have demonstrated that the method of images yields appropriate results. With the vertical wake structure showing a restricted expansion and an increased velocity deficit. However, at present the initial conditions measured during the experiments have not yet been implemented into the numerical model and thus comparisons can not be made. Currently the initial conditions for the model are generated using a potential flow model which is bounded using a multi-pole method [15].

Further work is required to apply the experimental initial conditions to the model. In addition the experimental results will be used to investigate the increase the lateral dissipation due the bounding conditions

9 Conclusions

Porous disc experiments have successfully been used to simulate the far wake region of MCECs, allowing investigation of the governing parameters affecting the wake structure and dissipation. It has been shown that the bounding effect of the free surface and sea bed act to restrict the expansion of the wake vertically. Further tests are planned to investigate the effects of:

- Water depth and proximity to the free surface
- Proximity to the sea bed – it is clear from initial results that sea bed shear may be influencing the mixing process.
- Ambient turbulence – this will have a major influence both on the structure of the initial condition and mixing process.

Experimental data will be fed into the eddy-viscosity model shortly. This will help drive the simulation development and it is expected that following some refinements the model will replicate a similar wake structure and recovery to that of the bounded porous disc experiments. Further refinements of the model are required, specifically in defining initial conditions and the global ambient eddy-viscosity term based on the ambient turbulence intensity.

Further investigations will seek to demonstrate the lateral expansion structure and to find a general shape relationship between the vertical and lateral components. This could then be used to optimise the computational effort.

Further experimental work packages of this project will focus upon measurement and simulation of larger scale horizontal axis rotors at a suitable test facility. Fully instrumented to measure rotor torque and power, wake characterisation around a single device will be followed by the study of interaction effects between multiple turbines.

Acknowledgements

This work is part of the DTI-funded project “Performance characteristics and optimisation of marine current energy converter arrays”, DTI project number T/06/00241/00/00.

References

- [1] Carbon Trust report, *UK, Europe and global tidal stream energy resource assessment*, Black and Veatch consulting, 2005.
- [2] N.O. Jensen, A note on wind generator interaction, RISO report RISO-M-2411, Roskilde, Denmark, 1983.

[3] L. Myers and A.S. Bahaj, Wake studies of a 1/30th scale horizontal axis marine current turbine, *Ocean Engineering*, V. 34, p 758-762, 2007.

[4] A.S. Bahaj, W.M.J. Batten, A.F. Molland and J.R. Chaplin, *Experimental investigation into the hydrodynamic performance of marine current turbines*, Sustainable Energy Series, Report 3, ISSN 1747-0544, March 2005.

[5] T. Burton, D. Sharpe, N. Jenkins, E. Bossanyi, *Wind Energy Handbook*, John Wiley & Sons, Ltd, 2001.

[6] European Commission, ‘The Exploitation of Tidal Marine currents’, Report EUR16683EN, 1996.

[7] *Offshore Installations: guidance on Design, construction and Certification*, UK Department of Energy, HMSO, London, Fourth Edition, 1990.

[8] DTI report, *Development, installation and testing of a large scale tidal current turbine*, Contract number T/06/0021/00/Rep, October 2005.

[9] P.M. Sforza, P. Sheerin and M. Smorto, Three-dimensional wakes of simulated wind turbines, *AIAA Journal*, V. 19, No. 9, p. 1101-1107, 1981.

[10] P.J. Bultjes, The interaction of windmill wakes, *Proceedings of the 2nd Int. Symposium on wind energy systems*, Amsterdam, 1978.

[11] J.R. Connel and R.L. George, The wake of the MOD-0A1 wind turbine at two rotor diameters downwind on 3 December 1981, Report no. PNL-4210, Pacific Northwest Laboratory, Battelle, U.S., 1982.

[12] P.E.J. Vermuelen, Mixing of simulated wind turbine wakes in turbulent shear flow, TNO report 79-09974, 1979.

[13] G. Voulgaris and J.H. Trowbridge, Evaluation of the Acoustic Doppler Velocimeter (ADV) for turbulence measurements, *Journal of atmospheric and oceanic technology*, V. 15, p. 272-289, 1998.

[14] S.J. McLelland and A.P. Nicholas, A new method for evaluating errors in high-frequency ADV measurements, *Hydrological Processes*. V. 14, p. 351-366, 2000.

[15] M.D. Thomson, The flow around marine current turbines, a dissertation submitted to the University of Bristol., 2004.